

Charmonium at BES and CLEO-c

T.Barnes

Physics Division ORNL, Oak Ridge, TN 37831, USA

Department of Physics and Astronomy, University of Tennessee, Knoxville TN 37996, USA

tbarnes@utk.edu

Abstract: This paper gives a short summary of some of the aspects of charmonium which can be addressed at BES and CLEO-c and other e^+e^- facilities. These topics include the spectroscopy of charmonium states, radiative transitions, e^+e^- widths, two-photon widths, hadron loop effects and open-flavor strong decays.

1 Introduction

Charmonium has been called the “hydrogen atom of QCD”, since many of the most characteristic and interesting aspects of QCD can be inferred from studies of the spectrum of charmonium states and their decays and interactions. Charmonium is a useful system for the study of forces between quarks in QCD, especially the poorly understood, nonperturbative confining interaction. This system is of special interest because the dynamics are only quasirelativistic, and the quark-gluon coupling at this mass scale is intermediate in strength; for this reason the more unusual features of QCD, such as relativistic corrections to the properties of bound states, spin-dependent forces from quark motion, virtual meson decay loops and various other effects may be only moderately large “controlled” corrections to a simple nonrelativistic potential model picture. Thus in charmonium we have a laboratory in which various novel dynamical effects may simultaneously be large enough to be clearly identified, and small enough so that they can be treated as perturbations of a familiar quantum mechanical model.

In this contribution we will discuss some of the aspects of charmonium that are most easily accessible at BES and CLEO-c. We will primarily discuss charmonium states above the open-charm threshold of 3.73 GeV, since these are quite poorly known; it should be straightforward to improve our knowledge in this area considerably. For our discussion we use a “generic” nonrelativistic potential model to generate the spectrum of states, and the resulting wavefunctions are used to evaluate electromagnetic transitions involving low-lying charmonium levels. We then discuss open-flavor strong decays of charmonium states, which is an important and largely unexplored topic. In our discussion we consider the properties of 1^{--} states in particular, as these are the most easily accessed at e^+e^- facilities.

2 A Generic Charmonium Potential Model

There are several charmonium potential models in the literature, which for the most part share the common features of short-ranged color Coulomb and long-ranged linear scalar confining potentials. In addition to this standard “Coulomb plus linear” potential, we also include a Gaussian-smeared spin-spin hyperfine term in our “zeroth-order potential”, since a careful treatment of the spin-spin force is important for the determination of the $^3S_1 - ^1S_0$ mass splittings. This issue has attracted recent attention due to the discovery of the η_c' by

BELLE [1] at a surprisingly high mass of $3654 \pm 6 \pm 8$ MeV (their average including inclusive production is 3639 ± 6 MeV), since confirmed by BABAR [2] (at $3630.8 \pm 3.4 \pm 1.0$ MeV) and CLEO [3] (at $3642.9 \pm 3.1 \pm 1.5$ MeV). The zeroth-order potential model Hamiltonian we assume is of the form

$$H_0 = \frac{\vec{p}^2}{m_c} - \frac{4\alpha_s}{3r} + br + \frac{32\pi\alpha_s}{9m_c^2} \tilde{\delta}_\sigma(r) \vec{S}_c \cdot \vec{S}_{\bar{c}} \quad (1)$$

where $\tilde{\delta}_\sigma(r) = (\sigma^3/\pi^{3/2}) \exp(-\sigma^2 r^2)$. Solution of the Schrödinger equation with this H_0 gives our zeroth-order charmonium wavefunctions. Splittings within an orbital multiplet are then determined by taking the matrix element of the spin-dependent Hamiltonian H_I between these zeroth-order wavefunctions. The spin-dependent Hamiltonian is taken from the one-gluon-exchange Breit-Fermi Hamiltonian (which gives spin-orbit and tensor terms) and an inverted spin-orbit (Thomas precession) term, which follows from the assumption of a Lorentz scalar confining interaction. This H_I is explicitly

$$H_I = \frac{2\alpha_s}{m_c^2 r^3} \vec{L} \cdot \vec{S} + \frac{4\alpha_s}{m_c^2 r^3} T - \frac{b}{2m_c^2 r} \vec{L} \cdot \vec{S}. \quad (2)$$

The assumption of a Lorentz scalar confining interaction is of course questionable; the nature of the spin-dependent contributions of the confining interaction to the interquark force is one of the interesting open questions which we hope to address in the study of charmonium.

There are four parameters in this simple potential model, the one-gluon-exchange coupling constant α_s (here for simplicity taken to be a constant), the string tension b , the charm quark mass m_c , and the contact hyperfine interaction smearing parameter σ . We have fixed these using an equal-weight fit to the masses of the 11 reasonably well established experimental charmonium states; the results are $\alpha_s = 0.5461$, $b = 0.1425$ GeV², $m_c = 1.4794$ GeV and $\sigma = 1.0946$ GeV, which gives an rms error of 13.6 MeV. (Of course no special meaning should be attached to these precise values, since the model is somewhat *ad hoc* and is at best only an approximate description of the physics of charmonium.) The experimental states used as input and the predictions for the $c\bar{c}$ spectrum (states below 4.2 GeV and all known 1^{--} states) are given in Table 3; these and some additional levels are shown in Fig.1.

It is evident in Fig.1 that the simple Coulomb plus linear potential model gives a very satisfactory fit to the known charmonium states. It is remarkable that both the mean level positions and the splittings within the 1S, 1P and 2S multiplets are well described, since they are testing different aspects of the interquark forces. The mean multiplet positions test the accuracy of the “funnel-shaped” potential, and determine approximate values for the two parameters α_s and b . The multiplet splittings in contrast test whether the spin-dependent interactions (spin-spin, spin-orbit and tensor) are also well described with the same parameters. These terms arise from the assumptions of transverse one-gluon exchange at short distances (which provides the J/ψ - η_c and ψ' - η_c' spin-spin splitting and dominates the P-wave splitting), and scalar confinement (which provides a negative spin-orbit term that is required for good agreement with the experimental χ_J masses). The general good agreement between the potential model and experiment is remarkable in view of the additional, presumably large effects such as virtual decay loops that have not been included in the model.

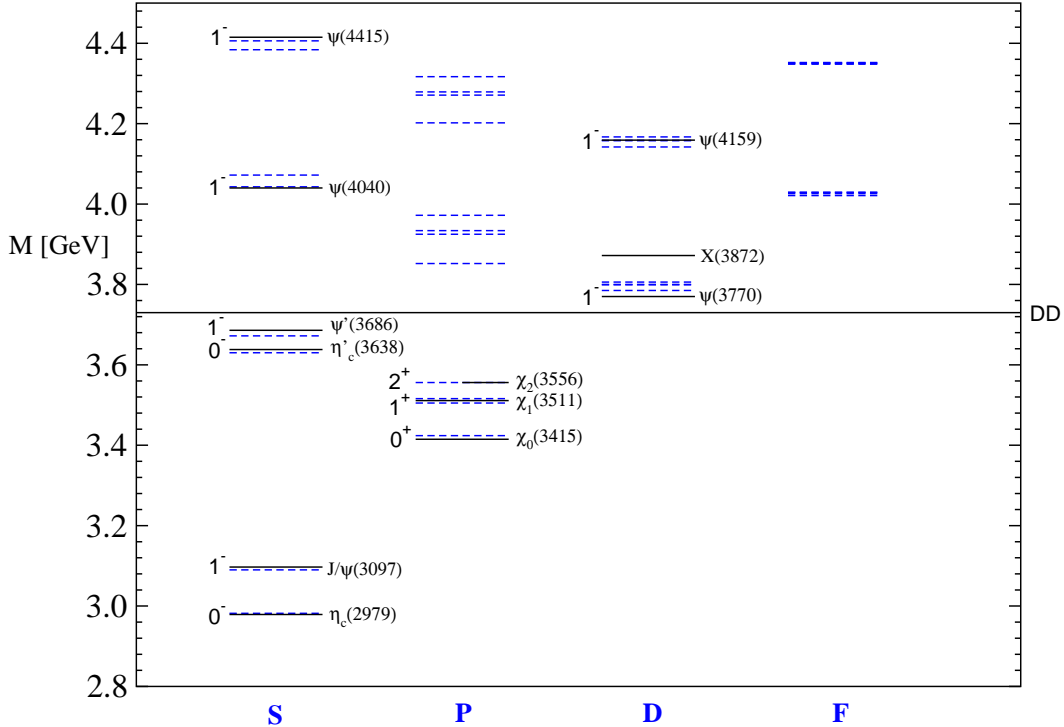


FIGURE 1. The spectrum of charmonium states predicted by the $c\bar{c}$ potential model described in the text, together with the 11 known experimental states. The X(3872) is also shown, although its identification with $c\bar{c}$ appears dubious.

We note in passing that lattice QCD has also been applied to charmonium, and predicts a very similar spectrum. (See for example the recent work of Liao and Manke [4].) It is very encouraging that the theoretically better-justified LQCD approach gives a pattern of energy levels which is very similar to the potential model; this supports our use of the more intuitive potential model to describe transitions involving charmonium states in this paper. We shall note however in our discussion of decays that virtual decay loops are expected to have important effects on both the spectrum and the composition of charmonium states [5,6], and these effects are neglected in pure $c\bar{c}$ potential models as well as in quenched LQCD.

3 Electromagnetic couplings

3.1 E1 radiative transitions

Radiative transitions are a very interesting feature of charmonium physics. They are quite straightforward to evaluate in $c\bar{c}$ potential models, and (with sufficient statistics) provide a route from the initial 1^{--} states produced in e^+e^- annihilation to $C = (+)$ charmonia.

The largest rates are for E1 (electric dipole) transitions, which we calculate using

$$\Gamma_{\text{E1}}(n^{2S+1}L_J \rightarrow n'^{2S'+1}L'_{J'} + \gamma) = \frac{4}{3} e_c^2 \alpha E_\gamma^3 \frac{E_f^{(c\bar{c})}}{M_i^{(c\bar{c})}} C_{fi} \delta_{SS'} |\langle n'^{2S'+1}L'_{J'} | r | n^{2S+1}L_J \rangle|^2. \quad (3)$$

Here $e_c = 2/3$ is the c -quark charge in units of $|e|$, α is the fine-structure constant, E_γ is the photon energy, and the angular matrix element C_{fi} is

$$C_{fi} = \max(L, L')(2J' + 1) \left\{ \begin{matrix} L' & J' & S \\ J & L & 1 \end{matrix} \right\}^2. \quad (4)$$

This formula is the same as that quoted by Ref.[7], except for our inclusion of a relativistic phase space factor of $E_f^{(c\bar{c})}/M_i^{(c\bar{c})}$. (This is usually not far from unity for the cases we consider.) To generate numerical results for transitions of particular interest to BES and CLEO-c, we have evaluated the matrix elements $\langle n'^{2S'+1}L'_{J'} | r | n^{2S+1}L_J \rangle$ using the nonrelativistic Schrödinger wavefunctions of the model described in the previous section. The resulting E1 rates are given in Table 4, together with the current experimental numbers.

Several very interesting features of E1 radiative transitions are evident in Table 4. First, the $1P \rightarrow 1S$ transitions are in very reasonable agreement with experiment. It is notable that the predicted radiative partial width for $h_c \rightarrow \gamma\eta_c$ is especially large, which suggests that decays to $\gamma\eta_c$ may provide a discovery channel for the elusive h_c . One possibility is $\gamma\gamma \rightarrow \eta_c'$, followed by the decay chain $\eta_c' \rightarrow \gamma h_c$, $h_c \rightarrow \gamma\eta_c$. Since these electromagnetic couplings are all reasonably well understood, detection of the h_c would simply be a matter of accumulating adequate statistics at a high-energy e^+e^- facility with sufficient $\gamma\gamma$ luminosity at $\sqrt{s} = 3.7$ GeV.

The theoretical rates for the $2S \rightarrow 1P$ transitions appear too large by about a factor of two, although the relativized model of Godfrey and Isgur [8] does not share this difficulty. We note in passing that good agreement between a pure- $c\bar{c}$ charmonium potential model and experiment may be spurious; decay loop effects will contribute two-meson continuum components to all these charmonium resonances, which may significantly modify the predicted radiative transition rates.

E1 radiative transitions from the higher-mass charmonium states are especially interesting. The 1^3D_1 candidate $\psi(3770)$ is predicted to have large partial widths to $\gamma\chi_1$ and $\gamma\chi_0$ (with branching fractions of 0.5% and 1.7% respectively), but the branching fraction to $\gamma\chi_2$ is predicted to be only about $2 \cdot 10^{-4}$. This small number however follows from the assumption that the $\psi(3770)$ is a pure 3D_1 state; if there is a significant admixture of S-wave basis states in the $\psi(3770)$,

$$|\psi(3770)\rangle = \cos(\theta) |^3D_1\rangle + \sin(\theta) |2^3S_1\rangle \quad (5)$$

one typically finds a much larger radiative width to $\gamma\chi_2$ [9,10]. (See Fig. 2. The sign of the mixing angle θ depends on the convention for the normalization of the 3D_1 and 2^3S_1 basis states; note for example in Fig.1 of Ref.[10] that a zero $\psi(3770) \rightarrow \gamma\chi_2$ width requires a small negative mixing angle, whereas with our conventions it would be positive.) Since the coupling of the $\psi(3770)$ to e^+e^- suggests a significant 2^3S_1 component, a measurement of this radiative partial width will be especially useful as an independent test of the presence of this amplitude in the $\psi(3770)$ wavefunction.

We note in passing that if the dominant mechanism of $^3D_1 - 2^3S_1$ basis state mixing in the $\psi(3686)$ and $\psi(3770)$ is through virtual charm meson decay loops such as DD , DD^* and D^*D^* , the assumption of a $2 \otimes 2$ orthogonal mixing matrix as in Eq.5 is incorrect. In this case the $\langle ^3D_1 | \psi(3686) \rangle$ and $\langle 2^3S_1 | \psi(3770) \rangle$ overlaps will no longer be simply related, and

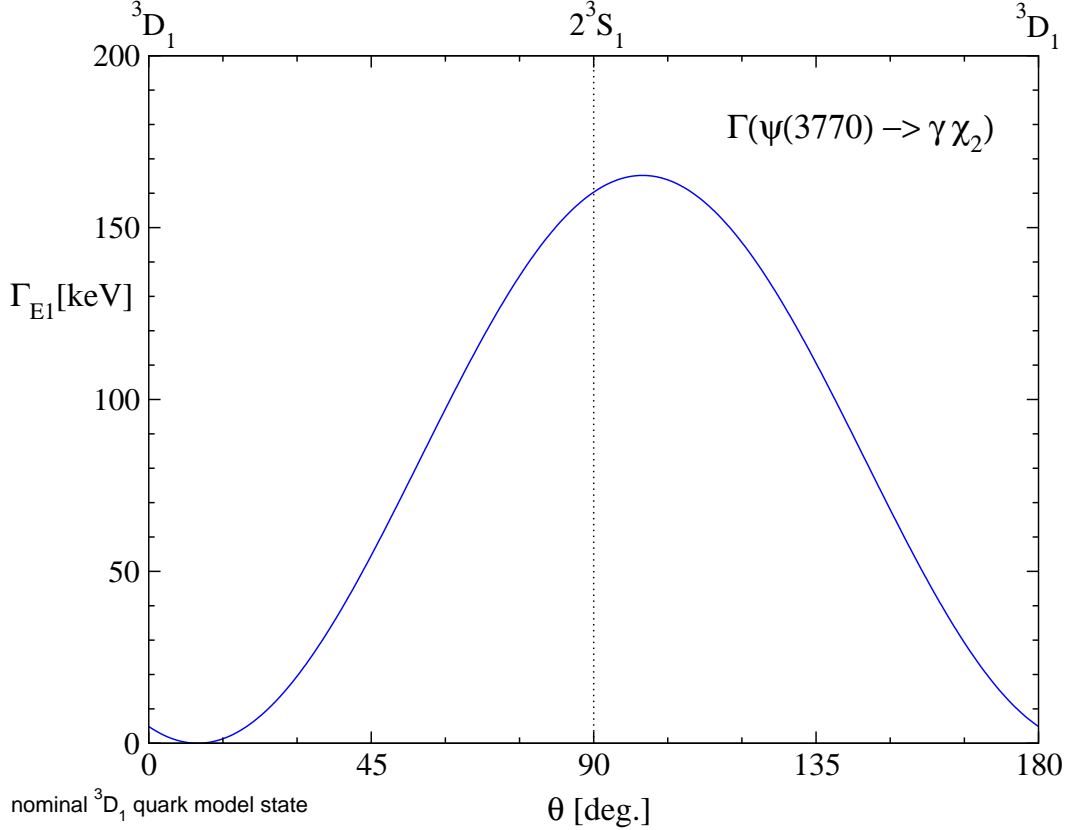


FIGURE 2. Predicted radiative partial width for the E1 transition $\psi(3770) \rightarrow \gamma\chi_2$ as a function of the 2^3S_1 - $3D_1$ mixing angle θ .

radiative transition amplitudes will also receive contributions from photon emission from the two-meson continua.

Next we consider radiative decays of the higher-mass vectors $\psi(4040)$ and $\psi(4159)$. As is evident in Table 4, if the $\psi(4040)$ is dominantly a 3^3S_1 state as we assume here, it should have very small E1 radiative widths to the triplet members of the 1P multiplet, with branching fractions of at most about 10^{-5} . The radiative widths to the unknown 2P triplet states are theoretically much larger, with branching fractions of 0.3 - $1 \cdot 10^{-3}$. Since the 2P states have large strong branching fractions to DD (χ_0 and χ_2) and DD* (χ_1 and χ_2) [11], it may be possible to identify these states in the DD and DD* invariant mass distributions of $\psi(4040) \rightarrow \gamma DD$ and γDD^* decays.

Radiative decays of the $\psi(4159)$ share certain features with the decays of both the $\psi(3770)$ and the $\psi(4040)$. As we found for the $\psi(4040)$, the E1 coupling of the $\psi(4159)$ to the 2P multiplet is much stronger than to the 1P multiplet, so radiative decays of the $\psi(4159)$ could be used to search for 2P states. The branching fraction to the 2^3P_0 χ_0 state in particular is predicted to be a relatively large 0.6%. A strong suppression of $\psi(4159)$ E1 decays to n^3P_2 states is predicted, as we found previously for the $\psi(3770)$. This again follows from the assumption that the state is purely D-wave $c\bar{c}$. Given an important S-wave component, which is suggested by the e^+e^- width, the coupling of the $\psi(4159)$ to n^3P_2 states should be much larger. Finally, a new feature is that one may reach the F-wave multiplet (specifically

the 3F_2 state) through the radiative decay of the $\psi(4159)$. Unfortunately this 3F_2 state is expected to be rather broad; we anticipate a total width of about 160 MeV, mainly to DD [11].

3.2 M1 radiative transitions

M1 transitions between charmonium states in pure $c\bar{c}$ models result from photon emission through the $H_I = -\vec{\mu} \cdot \vec{B}$ magnetic moment interaction of the c quark (and antiquark), and as such are suppressed relative to E1 transitions by the small factor of $1/m_c$ in the magnetic moment operator. The M1 transition amplitude is proportional to the matrix element of the spin operator, with a spatial factor that (without recoil corrections) is simply the matrix element of unity. M1 transitions are therefore nonzero only between states with the same $L_{c\bar{c}}$ (and different $S_{c\bar{c}}$, since the C-parity must change). If we assumed a spin-independent zeroth-order potential and neglect recoil effects, M1 transitions between different radial multiplets would vanish because the n^3S_1 and n^1S_0 states have orthogonal spatial wavefunctions. One such transition is actually observed in charmonium, $\psi' \rightarrow \gamma\eta_c$, which must be due in part to the nonorthogonal ψ' and η_c spatial wavefunctions and final meson recoil effects. The formula for M1 decay rates analogous to the E1 formula used in the previous section is

$$\Gamma_{M1}(n^{2S+1}L_J \rightarrow n'^{2S'+1}L'_{J'} + \gamma) = \frac{4}{3} e_c^2 \frac{\alpha}{m_c^2} E_\gamma^3 \frac{E_f^{(c\bar{c})}}{M_i^{(c\bar{c})}} \frac{2J'+1}{2L+1} \delta_{LL'} \delta_{S,S'\pm 1} \cdot |\langle n'^{2S'+1}L'_{J'} | n^{2S+1}L_J \rangle|^2. \quad (6)$$

Evaluating this formula for transitions from the ψ and ψ' gives the results shown in Table 1. A more detailed study of M1 radiative decay rates, incorporating recoil corrections (which are numerically important for transitions between multiplets such as $2S \rightarrow 1S$) will appear in Ref.[11].

TABLE 1. Theoretical and experimental M1 radiative partial widths of the ψ and ψ' , neglecting recoil effects.

Initial state	Final state	$\Gamma_{thy.}$ (keV)	$\Gamma_{expt.}$ (keV)
J/ψ	$\gamma\eta_c$	2.9	1.2 ± 0.3
ψ'	$\gamma\eta_c'$	0.21	
ψ'	$\gamma\eta_c$	4.6	0.8 ± 0.2
η_c'	$\gamma J/\psi$	7.9	

A well-known problem is evident in the decay rate $J/\psi \rightarrow \gamma\eta_c$, which is that the predicted rate in the nonrelativistic potential model is about a factor of 2-3 larger than experiment. Since this rate only involves the charm quark magnetic moment, and hence only its mass, this discrepancy is a surprise. The relativized Godfrey-Isgur model [8] predicts a somewhat smaller rate of 2.4 keV, which is still about a factor of two larger than experiment. Since the errors are rather large, it would clearly be very interesting to improve the experimental accuracy of this surprising partial width. If this discrepancy is confirmed, it may be an

indication that pure- $c\bar{c}$ models are a rather inaccurate description of charmonium, and that other components of the state vector such as two-meson continua make comparable important contributions to the M1 transition amplitudes. In view of the inaccuracy of the theoretical 1S M1 transition rate, it would also be interesting to test the 2S transition rate $\psi' \rightarrow \gamma\eta_c'$ experimentally. Unfortunately, this rate is predicted to be a rather small 0.21 keV in the nonrelativistic $c\bar{c}$ model.

An even larger discrepancy between experiment and theory is evident in the ‘‘hindered’’ M1 transition $\psi' \rightarrow \gamma\eta_c$. Since this rate is only nonzero due to recoil effects (not included here) and corrections to the naively orthogonal 1S and 2S $c\bar{c}$ wavefunctions, the discrepancy is perhaps less surprising than that found in the allowed 1S \rightarrow 1S $\psi \rightarrow \gamma\eta_c$ transition rate. In any case this is another example of an M1 transition rate in charmonium in which experiment and theory are clearly in disagreement. Since the experimental rate is again only about 4σ from zero, it would be very useful to improve the accuracy of this measurement at BES or CLEO-c.

M1 decays between charmonium resonances have only been observed between S-wave states. The rates between orbitally-excited states are typically predicted to be quite small, due to the small splittings within excited-L multiplets. They are large enough however to be observable given narrow initial states and large event samples. For example, a hypothetical 1D_2 $c\bar{c}$ assignment for the X(3872) could be tested through a search for its M1 decay to $\gamma\psi(3770)$, which has a partial width of 1.2 keV in our nonrelativistic potential model. The h_c (assumed at 3525 MeV) decay $h_c \rightarrow \gamma\chi_0$ has similar phase space, and is predicted to have a partial width of 0.8 keV. In contrast, the smaller phase space of the M1 transition from the higher-mass χ_2 state leads to an expected partial width for $\chi_2 \rightarrow \gamma h_c$ of only about 60 eV.

3.3 e^+e^- widths of 1^{--} states

Leptonic partial widths are trivially accessible at e^+e^- machines, and they provide interesting (and currently rather puzzling) information regarding the wavefunctions of 1^{--} charmonium states. In the nonrelativistic $c\bar{c}$ potential model e^+e^- annihilation through the photon couples to the $c\bar{c}$ pair at contact, so these widths are only predicted to be nonzero for S-wave $c\bar{c}$ systems. This nonrelativistic partial width is given by the van Royen - Weisskopf formula [12],

$$\Gamma_{c\bar{c}}^{e^+e^-}(^3S_1) = \frac{16}{9} \alpha^2 \frac{|\psi(0)|^2}{M_{c\bar{c}}^2} \quad (7)$$

where the radial wavefunction is normalized to $\int_0^\infty r^2 dr |\psi(r)|^2 = 1$. Strictly speaking, for relativistic bound states the annihilation is not completely local, so some coupling of D-wave states to e^+e^- is predicted. This width at leading order is proportional to $|\psi''(0)|^2$,

$$\Gamma_{c\bar{c}}^{e^+e^-}(^3D_1) = \frac{50}{9} \alpha^2 \frac{|\psi''(0)|^2}{M_{c\bar{c}}^2 m_c^4} \quad (8)$$

which is much smaller than the corresponding widths of the 3S_1 states. Evaluating these widths using the nonrelativistic quark model wavefunctions described here gives the results quoted in Table 2.

Note that the agreement between the model and experiment is not especially good. This may be in part due to the choice of parameters, although the overestimate of the J/ψ

TABLE 2. Predictions of the nonrelativistic $c\bar{c}$ potential model for e^+e^- partial widths, together with current PDG experimental values [13].

State	Asst.	$\Gamma_{thy.}^{e^+e^-}$ (keV):	$\Gamma_{expt.}^{e^+e^-}$ (keV):
J/ψ	1^3S_1	12.13	5.40 ± 0.17
ψ'	2^3S_1	5.03	2.12 ± 0.12
$\psi(3770)$	1^3D_1	0.056	0.26 ± 0.04
$\psi(4040)$	3^3S_1	3.48	0.75 ± 0.15
$\psi(4159)$	2^3D_1	0.096	0.77 ± 0.23
$\psi(4415)$	4^3S_1	2.63	0.47 ± 0.10

leptonic width by roughly a factor of two seems to be a common difficulty in naive potential models. Non-valence components in the charmonium states, such as $c\bar{c}g$ or D meson pairs from decay loops, may also contribute to this inaccuracy. Concerns have also been expressed that the leading-order QCD radiative corrections may be large [14], which could significantly reduce the overall scale of the leptonic widths. Of course the leading-order corrections are prescription-dependent, so it is not clear that this claim is reliable. In any case it is evident that a simple change of scale will not resolve the discrepancies in Table 2, since the nominally D-wave states $\psi(3770)$ and $\psi(4159)$ both have significant leptonic widths.

The large experimental leptonic widths of the $\psi(3770)$ and $\psi(4159)$ relative to predictions for pure D-wave $c\bar{c}$ states (see Table 2) may be due to an admixture of an S-wave $c\bar{c}$ component [9,10]. As we noted previously, this mixing can be tested through measurements of the E1 radiative decay rates $\psi(3770) \rightarrow \gamma\chi_2$ and (with more difficulty) $\psi(4159) \rightarrow \gamma\chi_2$ and $\gamma\chi_2'$, since these transitions are very sensitive to the presence of S-wave $c\bar{c}$ components. Radiative width ratios such as $\Gamma(\psi(3770) \rightarrow \gamma\chi_2)/\Gamma(\psi(3770) \rightarrow \gamma\chi_1)$ and the leptonic width ratio $\Gamma(\psi(3770) \rightarrow e^+e^-)/\Gamma(\psi' \rightarrow e^+e^-)$ provide two independent tests of S-D mixing.

3.4 Two-photon couplings

Although neither BES nor CLEO-c will have adequate \sqrt{s} to usefully exploit two-photon production of charmonium resonances, this has been a useful technique at higher-energy e^+e^- facilities, which we briefly mention here in the interest of completeness. This subject has been reviewed elsewhere [15].

Two-photon resonance production involves the reaction $e^+e^- \rightarrow e^+e^-R$, $R \rightarrow f$, where R is a $C = (+)$ meson resonance and f is the exclusive final state observed. This process proceeds dominantly through the two-photon coupling of the resonance, $e^+e^- \rightarrow e^+e^-\gamma\gamma$, $\gamma\gamma \rightarrow R$, and hence implicitly gives the two-photon partial width $\Gamma_{\gamma\gamma}(R)$ times the branching fraction $B(R \rightarrow f)$. One may also consider the case of one or both photons significantly off mass shell $q_\gamma^2 \neq 0$, which gives the generalized widths $\Gamma_{\gamma^*\gamma}(R)$ and $\Gamma_{\gamma\gamma^*}(R)$. The interesting question for off-shell widths is whether they are given by a vector dominance formula with the mass of the relevant vector, in this case the J/ψ .

In the limit of large quark mass (and hence a zero-range charm quark propagator) the two-photon width of an S-wave charmonium state is proportional to the wavefunction at contact

squared. In this approximation, higher-L states are produced with amplitudes proportional to the L^{th} derivative of the wavefunction at contact [16]. (In practice this attractively simple contact approximation appears marginal at best at the $c\bar{c}$ mass scale.) Both the η_c and η_c' have been seen in two-photon collisions; the $\gamma\gamma$ width of the η_c is approximately 7 keV, comparable to quark model expectations. The $\eta_c' \rightarrow \gamma\gamma$ width is not known because one measures the $\gamma\gamma$ width times the branching fraction to an exclusive final state, and the η_c' absolute branching fractions are not known. Higher-L $c\bar{c}$ two-photon widths are suppressed by the mass of the charm quark, and therefore are not very well established; only the P-wave χ_0 and χ_2 states have been observed. The theoretical ratio of P-wave $\gamma\gamma$ widths in the large quark mass limit is $\Gamma_{\gamma\gamma}(^3P_0)/\Gamma_{\gamma\gamma}(^3P_2) = 15/4$, however this may be modified significantly by QCD radiative corrections and finite quark mass effects. Nonrelativistically the $\gamma\gamma$ state produced by the 3P_2 should be pure helicity two; relativistic corrections are expected to give rise to a small helicity-zero $\gamma\gamma$ component as well.

Although one can in principle produce higher-L $c\bar{c}$ states in $\gamma\gamma$ collisions, in practice these rates fall rapidly with increasing L for $c\bar{c}$ and heavier $Q\bar{Q}$ systems. As an example, the two-photon width of a hypothetical $^1D_2(3840)$ $c\bar{c}$ state is predicted to be only 20 eV [15].

4 Open-charm strong decays

The dominant decay modes of most hadrons are open-flavor strong decays, in which the initial quarks separate into different final states. Despite their importance in QCD, these open-flavor decays are not at all well understood on a fundamental level. There are very exciting prospects for greatly improving our understanding of this important aspect of non-perturbative QCD through studies of the open-flavor decays of charmonium states above the DD threshold.

Strong decay couplings are also of great interest because at second-order they give rise to $(c\bar{c}) \rightarrow (c\bar{q})(q\bar{c}) \rightarrow (c\bar{c})$ loop diagrams, which are not included in pure $c\bar{c}$ potential models or in quenched lattice gauge theory. As these virtual decay loop effects are believed to be numerically important in charmonium [5,6], it is correspondingly important to improve our understanding of the strong decay couplings that drive these processes. This will be most straightforward through studies of the decay couplings of $c\bar{c}$ states above open-charm threshold.

At present these open-flavor decays are treated using simple quark model descriptions of the decay process, which are known to give numerically reasonable results for many light hadron decays. The earliest of these decay models is the “ 3P_0 model” of Micu [17] and LeYaouanc *et al.* [18], who describe the decay in terms of the local production of a new $q\bar{q}$ with 0^{++} quantum numbers (hence 3P_0). The overall strength of this dimensionless pair production amplitude γ is simply fitted to experiment, and for light mesons is found to be $\gamma \approx 0.4$ [19].

The best known theoretical work on charmonium is the series of papers by the Cornell group [20,21,22,23], which includes a study of open-flavor strong decays [23]. Remarkably, the strong decay model assumed by the Cornell group is *not* the standard 3P_0 model. Instead, they assume that strong decays take place through pair production from the linear confining potential, which they assume to transform as the time component of a Lorentz vector, γ_0 . (Vector confinement was assumed in some hadron models in the 1980s, but has since been

largely replaced by the assumption of Lorentz scalar confinement.)

A more recent study of possible QCD strong decay mechanisms by Ackleh *et al.* [24] found that the 3P_0 model decay amplitudes were quite similar in form to what one would find for pair production by the linear scalar confining interaction, although the usual string tension leads to an overestimated decay amplitude by about a factor of 2-3 for light meson decays.

These two models of the decay interaction, Lorentz vector versus Lorentz scalar, will give different predictions for open-flavor strong decay amplitudes that can be tested at BES and CLEO-c. Unfortunately the Cornell group did not give detailed amplitude decompositions for their Lorentz vector decay model; instead they evaluated a “resolvent” that gave the cross section ratio R , and showed graphical results for R and the branching fractions. The required evaluation of decay amplitudes in this model is in progress [25]. Similarly, the corresponding 3P_0 decay model amplitudes have (remarkably) never been evaluated in detail for the higher charmonium states. This work has now largely been completed [11], and some of the results are presented here. In particular we will discuss results specific to the easily accessible 1^{--} states.

The results we find for the open-charm decay modes of the four accessible 1^{--} states in the 3P_0 model, with SHO wavefunctions and parameters of $\beta = 0.5$ GeV (length scale) and $\gamma = 0.4$ (pair production amplitude) are shown in Table 5. The lightest state is the $\psi(3770)$, which is usually considered a 3D_1 state, can only decay to DD; it is predicted to have a total width of 43 MeV, about twice the experimental value. The total widths of the nominally 3^3S_1 $\psi(4040)$ and 2^3D_1 $\psi(4159)$ are both predicted to be rather near the PDG experimental values [13]; 74 MeV (theory) versus 52 ± 10 MeV (experiment) for the $\psi(4040)$, and 73 MeV (theory) versus 78 ± 20 MeV (experiment) for the $\psi(4159)$.

The branching fractions of the $\psi(4040)$ are a famous problem; although phase space favors DD over DD^* , and D^*D^* has essentially no phase space, the existing data actually suggests that the relative branching fractions are $D^*D^* \gg DD^* \gg DD$. (The ratios quoted by Mark I at SLAC were $32.0 \pm 12.0 : 1 : 0.05 \pm 0.03$ [13,26].) The 3P_0 model is at least partially in agreement here, as is the Cornell decay model [23], since both predict a very small DD mode. (In the decay models this is a result of a node in the decay amplitude of the radially-excited 3^3S_1 state.) The Cornell decay model however predict comparable branching fractions to DD^* and D^*D^* . The 3P_0 model with our parameters finds a similar result (see Table 5), although there is a node in the DD^* decay amplitude that can also significantly reduce the DD^* branching fraction [11]. It would be very interesting to measure and recalculate these branching fractions carefully to determine whether there is indeed disagreement with theoretical expectations. Note also that the D^*D^* mode is especially interesting, in that there are three amplitudes in this final state, 1P_1 , 5P_1 and 5F_1 . The 3P_0 model predicts that decays from S-wave $c\bar{c}$ states have zero 5F_1 amplitudes, and that the ratio of the two P-wave amplitudes is $^5P_1/^1P_1 = -2\sqrt{5}$.

The 2^3D_1 candidate $\psi(4159)$ has the same modes accessible as the $\psi(4040)$, but is predicted to have a very different pattern of branching fractions and decay amplitudes. The mode DD^* is theoretically strongly suppressed, DD should be large, and D^*D^* should be the leading mode. The relative amplitudes within the D^*D^* final state are predicted to have a very characteristic pattern; 5F_1 is predicted to be dominant, and 1P_1 is predicted to be larger than 5P_1 , in the ratio $^1P_1/^5P_1 = -\sqrt{5}$.

Finally, the $\psi(4415)$ is assigned to 4^3S_1 in potential models. This highly radially-excited level has several decay amplitude nodes that make the predicted decay branching fractions less reliable. The expected dominant mode among S-wave pairs is D^*D^* , with the same amplitude ratios quoted above for the 3^3S_1 state.

An interesting new feature of $\psi(4415)$ decays is that there is sufficient phase space for decays to S+P D-meson pairs; in particular, the interesting new CLEO states $D_{sJ}^*(2317)$ and $D_{s1}(2460)$ can both be made in S-wave (assuming that the $D_{sJ}(2317)$ is a scalar), in $\psi(4415) \rightarrow D_s^*D_{sJ}^*(2317)$ and $\psi(4415) \rightarrow D_sD_{s1}(2460)$ respectively. (Nominally these decay modes are just above threshold, but they are accessible once the width of the $\psi(4415)$ is incorporated.) Since the branching fractions expected to these final states are not especially small [11], the $\psi(4415)$ could provide a straightforward source of a large sample of $D_{sJ}^*(2317)$ and $D_{s1}(2460)$ events.

5 Conclusions

In this note we have reviewed some topics of current interest in charmonium which can be addressed at the BES and CLEO-c facilities. The topics discussed here were electromagnetic couplings and decays (E1, M1, e^+e^- and two-photon), hadron decay loops and open-flavor strong decays. Studies of properties of the $\psi(3770)$, $\psi(4040)$ and $\psi(4159)$ are especially interesting in this regard. The E1 decays of the $\psi(3770)$, in particular to $\gamma\chi_2$, can be compared with the e^+e^- width to allow tests of S-D mixing, which may be due to open-flavor decay loops. The relative strong branching fractions of the $\psi(4040)$ and the $\psi(4159)$ to DD , DD^* and D^*D^* , and in particular the relative size of the three D^*D^* decay amplitudes, allow sensitive tests of strong decay models. Finally, the high-mass tail of the $\psi(4415)$ may be useful as a source of events containing the new narrow resonances $D_{sJ}^*(2317)$ and $D_{s1}(2460)$.

Acknowledgments

I would like to thank the organizers of the Beijing BES/CLEO-c joint workshop, in particular Wei-Guo Li and Ian Shipsey, for their kind invitation to review aspects of charmonium at this meeting, and for the opportunity to discuss physics with my fellow participants. This report is an extended version of material presented at the workshop. I am also grateful to F.E.Close, S.Godfrey, J.Quigg, J.Rosner and E.S.Swanson for discussions of various aspects of the material presented here.

References

- [1] S. K. Choi *et al.* [BELLE collaboration], Phys. Rev. Lett. **89**, 102001 (2002) [Erratum-ibid. **89**, 129901 (2002)] [arXiv:hep-ex/0206002].
- [2] B. Aubert *et al.* [BABAR Collaboration], arXiv:hep-ex/0311038.
- [3] J. Ernst *et al.* [CLEO Collaboration], arXiv:hep-ex/0306060.
- [4] X. Liao and T. Manke, arXiv:hep-lat/0210030.
- [5] E. van Beveren, C. Dullemond and G. Rupp, Phys. Rev. D **21**, 772 (1980) [Erratum-ibid. D **22**, 787 (1980)].

- [6] K. Heikkila, S. Ono and N. A. Tornqvist, Phys. Rev. D **29**, 110 (1984) [Erratum-ibid. D **29**, 2136 (1984)].
- [7] W. Kwong and J. L. Rosner, Phys. Rev. D **38**, 279 (1988).
- [8] S. Godfrey and N. Isgur, Phys. Rev. D **32**, 189 (1985).
- [9] J. L. Rosner, Phys. Rev. D **64**, 094002 (2001) [arXiv:hep-ph/0105327].
- [10] J. L. Rosner, arXiv:hep-ph/0405196.
- [11] T.Barnes, S.Godfrey and E.S.Swanson (in preparation).
- [12] R. Van Royen and V. F. Weisskopf, Nuovo Cim. A **50**, 617 (1967) [Erratum-ibid. A **51**, 583 (1967)].
- [13] S.Eidelman *et al.*(Particle Data Group), Phys. Lett. B **592**, 1 (2004).
- [14] R. Barbieri, R. Gatto, R. Kogerler and Z. Kunszt, Phys. Lett. B **57**, 455 (1975).
- [15] T. Barnes, “Two photon couplings of quarkonia with arbitrary J(PC),” *Int. Workshop on Photon-Photon Collisions, La Jolla, CA, Mar 22-26, 1992.*
<http://www.slac.stanford.edu/spires/find/hep/www?r=ornl-ccip-92-05>
- [16] E. S. Ackleh, T. Barnes and F. E. Close, Phys. Rev. D **46**, 2257 (1992).
- [17] L. Micu, Nucl. Phys. B **10**, 521 (1969).
- [18] A.LeYaouanc, L.Oliver, O.Pène and J.Raynal, Phys. Rev. D **8**, 2223 (1973); *ibid.*, D9, 1415 (1974); D11, 680 (1975); D11, 1272 (1975); Phys. Lett. **71B**, 397 (1977).
- [19] T. Barnes, F. E. Close, P. R. Page and E. S. Swanson, Phys. Rev. D **55**, 4157 (1997) [arXiv:hep-ph/9609339].
- [20] E. Eichten, K. Gottfried, T. Kinoshita, J. B. Kogut, K. D. Lane and T. M. Yan, Phys. Rev. Lett. **34**, 369 (1975) [Erratum-ibid. **36**, 1276 (1976)].
- [21] E. Eichten, K. Gottfried, T. Kinoshita, K. D. Lane and T. M. Yan, Phys. Rev. Lett. **36**, 500 (1976).
- [22] E. Eichten, K. Gottfried, T. Kinoshita, K. D. Lane and T. M. Yan, Phys. Rev. D **17**, 3090 (1978) [Erratum-ibid. D **21**, 313 (1980)].
- [23] E. Eichten, K. Gottfried, T. Kinoshita, K. D. Lane and T. M. Yan, Phys. Rev. D **21**, 203 (1980).
- [24] E. S. Ackleh, T. Barnes and E. S. Swanson, Phys. Rev. D **54**, 6811 (1996) [arXiv:hep-ph/9604355].
- [25] E.S.Swanson (in preparation).
- [26] G. Goldhaber *et al.*, Phys. Lett. B **69**, 503 (1977).

TABLE 3. Predictions of the nonrelativistic $c\bar{c}$ potential model discussed in the text for the charmonium spectrum to 4.2 GeV (and for all S-wave states to 4.5 GeV).

State	Mass (MeV):	Expt. (input)	Theor.
J/ ψ		3097	3090
η_c		2979	2982
ψ'		3686	3672
η_c'		3638	3630
$\psi(3^3S_1)$		4040	4072
$\eta_c(3^1S_0)$			4043
$\psi(4^3S_1)$		4415	4406
$\eta_c(4^1S_0)$			4384
χ_2		3556	3556
χ_1		3511	3505
χ_0		3415	3424
h_c			3516
$\chi_2(2^3P_2)$			3972
$\chi_1(2^3P_1)$			3925
$\chi_0(2^3P_0)$			3852
$h_c(2^1P_1)$			3934
$\psi_3(3^3D_3)$			3806
$\psi_2(3^3D_2)$			3800
$\psi(3^3D_1)$		3770	3785
$\eta_{c2}(1^3D_2)$			3799
$\psi_3(2^3D_3)$			4167
$\psi_2(2^3D_2)$			4158
$\psi(2^3D_1)$		4159	4142
$\eta_{c2}(2^1D_2)$			4158
$\chi_4(3^3F_4)$			4021
$\chi_3(3^3F_3)$			4029
$\chi_2(3^3F_2)$			4029
$\eta_{c3}(1^3F_3)$			4026

TABLE 4. Theoretical and experimental E1 radiative partial widths of the easily accessible 1^{--} states, as well as some interesting additional cases (see text). The experimental $\psi(3770)$ numbers are taken from Ref.[10].

Initial state	Final state	$\Gamma_{thy.}$ (keV)	$\Gamma_{expt.}$ (keV)
χ_2	$\gamma J/\psi$	424	426 ± 48
χ_1	$\gamma J/\psi$	320	288 ± 51
χ_0	$\gamma J/\psi$	155	119 ± 17
h_c	$\gamma \eta_c$	494	
ψ'	$\gamma \chi_2$	38	18.0 ± 2.0
	$\gamma \chi_1$	54	23.6 ± 2.7
	$\gamma \chi_0$	62	24.2 ± 2.5
η_c'	γh_c	49	
$\psi(3^3S_1)(4040)$	$\gamma \chi_2$	0.5	
	$\gamma \chi_1$	0.4	
	$\gamma \chi_0$	0.2	
	$\gamma \chi_2(2^3P_2)$	14	
	$\gamma \chi_1(2^3P_1)$	39	
	$\gamma \chi_0(2^3P_0)$	54	
$\psi(3^3D_1)(3770)$	$\gamma \chi_2$	4.9	≤ 330 (90% c.l.)
	$\gamma \chi_1$	126	280 ± 100
	$\gamma \chi_0$	405	320 ± 100
$\psi(2^3D_1)(4159)$	$\gamma \chi_2$	0.8	
	$\gamma \chi_1$	14	
	$\gamma \chi_0$	27	
	$\gamma \chi_2(2^3P_2)$	5.9	
	$\gamma \chi_1(2^3P_1)$	168	
	$\gamma \chi_0(2^3P_0)$	485	
	$\gamma \chi_2(3^3F_2)$	51	

TABLE 5. Open-charm strong decay modes of the 1^{--} states accessible at BES and CLEO-c. A reaction-dependent factor has been removed from the decay subamplitudes in the final column of the table, so only the amplitude ratios are physically meaningful.

State	Mode	$\Gamma_{expt.}$ (MeV)	$\Gamma_{thy.}$ (MeV)	Subamps.
$\psi(3770)$ (3D_1)	DD		43.	
	all	23.6 ± 2.7	43.	
$\psi(4040)$ (3^3S_1)	DD		0.1	
	DD*		33.	
	$D_s D_s$		8.	
	$D^* D^*$		33.	$^1P_1 = +0.056$ $^5P_1 = -0.251$ $^5F_1 = 0$
	all	52 ± 10	74.	
$\psi(4159)$ (2^3D_1)	DD		16.	
	DD*		0.4	
	$D^* D^*$		35.	$^1P_1 = +0.081$ $^5P_1 = -0.036$ $^5F_1 = -0.141$
	$D_s D_s$		8.	
	all	78 ± 20	73.	
$\psi(4415)$ (4^3S_1)	DD		0.4	
	DD*		2.3	
	$D^* D^*$		16.	$^1P_1 = -0.018$ $^5P_1 = +0.081$ $^5F_1 = 0$
	$D_s D_s$		1.3	
	$D_s D_s^*$		2.6	
	$D_s^* D_s^*$		0.7	$^1P_1 = +0.006$ $^5P_1 = -0.028$ $^5F_1 = 0$
	S+P modes [11]			
	all	52 ± 10		